ANALYSIS OF GER IMAGING SPECTROMETER DATA ACQUIRED DURING THE EUROPEAN IMAGING SPECTROMETRY AIRCRAFT CAMPAIGN (EISAC) '89. QUALITY ASSESSMENTS AND FIRST RESULTS

Joachim Hill

Institute for Remote Sensing Applications, Laboratory for Image Processing
Commission of the European Communities, Joint Research Centre, I-21020 Ispra (Va), Italy

Abstract

During the European Imaging Spectrometry Aircraft Campaign (EISAC) '89 airborne imaging spectrometer data (GER 63-Band Multi-Spectral Scanner, Moniteq FLI/PMI) have been acquired over 6 different test sites. The Joint Research Centre (JRC, LIP/IRSA) has taken this opportunity to initiate an own experiment on the use of High Resolution Spectrometer data in land degradation and soil erosion hazard assessment. The GER 63- Channel Imaging Spectrometer (GERIS) was flown twice over a test site in the Southern Ardèche region (France), while ground information was collected by JRC scientists and collaborating institutes.

The radiometric quality of GERIS data has been analyzed by using several images acquired during the EISAC '89 campaign (Freiburg, FRG, Adria, Italy and Ardèche, France). The results indicate that instrument related problems (in-flight calibration, band setting, bandwidth and signal-to- noise ratio) will complicate the analysis of data especially from the first two spectrometers (0.45-0.88 µm and 1.2-1.8 µm). Pre-flight specifications seem to be met in a better way with the second short-wave infrared spectrometer (2.0 - 2.5 µm). In this spectral range, identical absorption features have been detected in the airborne data as well as in the radiometric field and laboratory measurements which correspond to the mineral content of soil and rock samples from the study region.

1. INTRODUCTION

In May/June 1989 a European Imaging Spectrometry Aircraft Campaign (EISAC) was carried out in which two airborne imaging spectrometers (Moniteq FLI/PMI, GER Imaging Spectrometer (GERIS) 63-channel Scanner) have been flown over different ocean and land application test sites. As an extension to EISAC'89 additional flights with the GERIS instrument were carried out, one of which took place over a JRC test site in the southern Département Ardèche, France.

The objective of this study in an analysis of the radiometric characteristics of GERIS data which have been acquired during the 1989 flight campaign in Europe. It invloves assessments of the radiometric in-flight calibration, spectral bandwidth, position of the spectral channels and the signal-to-noise ratio, all of which may affect thematic evaluations of the imaging spectrometer data.

2. THE GER 63-CHANNEL IMAGING SPECTROMETER (GERIS)

On demand from mining and petroleum industries, the Geophysical and Environmental Research Corporation (GER) has developed a 63-channel high spectral resolution scanner for commercial use (a 64th channel is used to store aircraft gyroscopic information) which was meanwhile flown during various survey missions in the U.S.A. and Australia (Mackin and Munday 1988; Kruse *et al.* 1990; Lee *et al.* 1990). The system consists of three grating spectrometers with individual line detector arrays, and it simultaneously acquires 63 inherently co-registred data channels (Lehmann *et al.* 1989). In order to provide maximum signal-to-noise, the spectral bands vary in width across the spectrum (Table 1).

TABLE 1
GERIS BAND SPECIFICATIONS FOR EISAC '89

Wavelength Range	Module	Number of Channels	Sampling Interval
0.477–0.843 μm	VIS/NIR	31	12.3 nm
1.44–1.80 μm	SWIR I	4	120 nm
2.005–2.443 μm	SWIR II	28	16.2 nm

Source: Lehmann et al.(1989)

TABLE 2
GERIS FLIGHTS ARDÈCHE, 29 JUNE 1989

	Track 1	Track 2
Location	44.4° N / 4.25° E	44.4° N / 4.25° E
Acquisition Time	12.20 GMT	12.30 GMT
Aircraft Altitude	3350 m amsl	3350 m amsl
Aircraft Heading	40.0 degr	323.0 degr
Sun Elevation	67.86 degr	67.12 degr
Sun Azimuth	201.1 degr	206.9 degr

The GERIS was flown on a Piper Aztec twin engine aircraft at an average altitude of 3,000 m above ground level. A 90 degree scan provides a swath width of 512 pixels which, given an IFOV of 3.3 mrad, represent ground resolution elements of nominally 10 x 10 meters. The GERIS raw data have been system-corrected at the German Aerospace Research Establishment (DLR), which comprised corrections for aircraft roll, detector speed and scanning angles. No data have been collected in band 28 (0.811 μm), probably due to a failure of the detector element (Lehmann *et al.* 1989).

3. THE ARDÈCHE HIGH RESOLUTION SPECTROMETRY EXPERIMENT

The study site for JRC's experiment on the use of high resolution spectrometer data in "Land Degradation and Soil Erosion Hazard Assessment" is located in the southern· Département Ardèche, France (Plaine de Berrias-Beaulieu) (Fig. 1)

Morphology and land-use of the area are strongly influenced from the tectonic fault pattern and contrasting petrography of limestones, marlstones and fluvial sediments (Negendank *et al.* 1990). The agricultural use is mainly limited to the alluvial plain of the river Chassezac, with some extension into the marlstone block being located to the east. These marls form the transition to a wooded, NE/SW striking, cretacious limestone ridge (Fig. 2).

According to FAO nomenclature (FAO, 1988), most soils in the study region fall into the category of leptosols, being limited in depth by continuous hard rock or highly calcareous material. Also the fluvisols contain significant amounts of calcareous constituents, and there is only isolated occurrence of cambisols which have developed on accumulated fine material (Riezebos *et al.* 1990). Calcite and quartz are the dominant mineral constituents in most soils, the main accessories are feldspars, kaolinite and illite (Negendank *et al.* 1990).

The natural vegetation typically comprises sub-mediterranean forests, garrigue areas and rangelands, the latter representing different stages of vegetative regeneration. Especially the marlstone area includes extended locations which exhibit the results of frequently occurring, severe soil erosion hazards (badlands).

Imaging spectrometer data provide spectral information which can be used to remotely identify many rocks and minerals, some plant species and physiological characteristics of vegetation (Vane and Goetz 1985). The Ardèche site appears to be an excellent area for testing the application of HRS technology to mineral mapping in soils and exposed rocks, to study the influence of variable vegetation cover on the recognition of soil components, and to compare

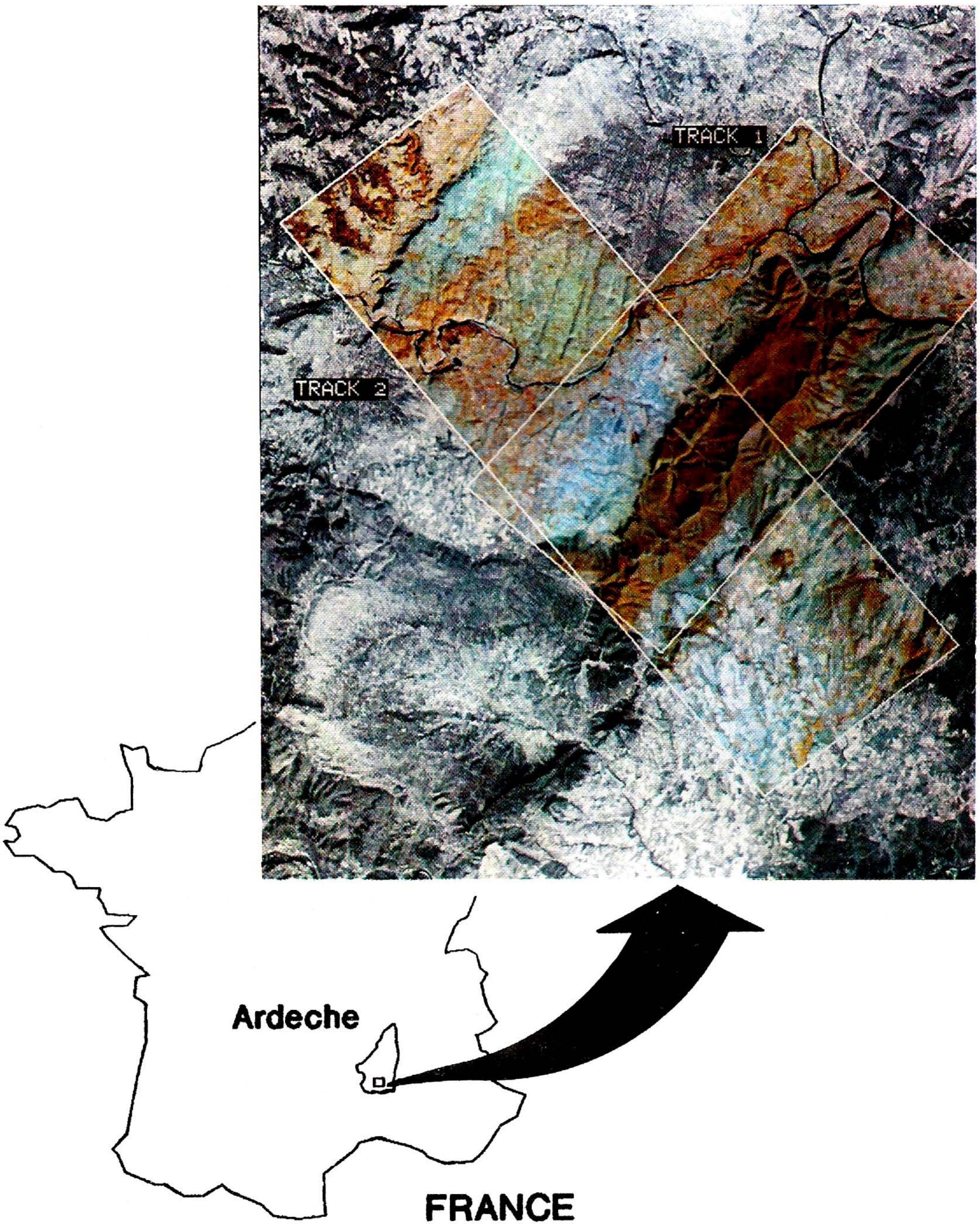

Fig. 1. GERIS flight tracks in the Ardèche High Resolution Spectrometry test site, presented as merge of geocoded TM bands 4-5-3 (colour) and SPOT band XS2 (b&w), both images acquired on 29 September 1986.

spectral indicators with the results from the geoscientific laboratory analysis.

The GERIS instrument was flown over the Ardèche site during 26 June 1989, and data were acquired within two tracks (Table 2). Radiometric ground measurements have been conducted during the overpass (Maracci *et al.* 1990; Lehmann *et al.* 1989), additional reflectance measurements of soil and rock surface samples were performed in the laboratory (Lehmann *et al.* 1989), and the mineral content of these samples was analyzed by means of X-ray diffraction (Negendank *et al.* 1990). After the flight, geologic and

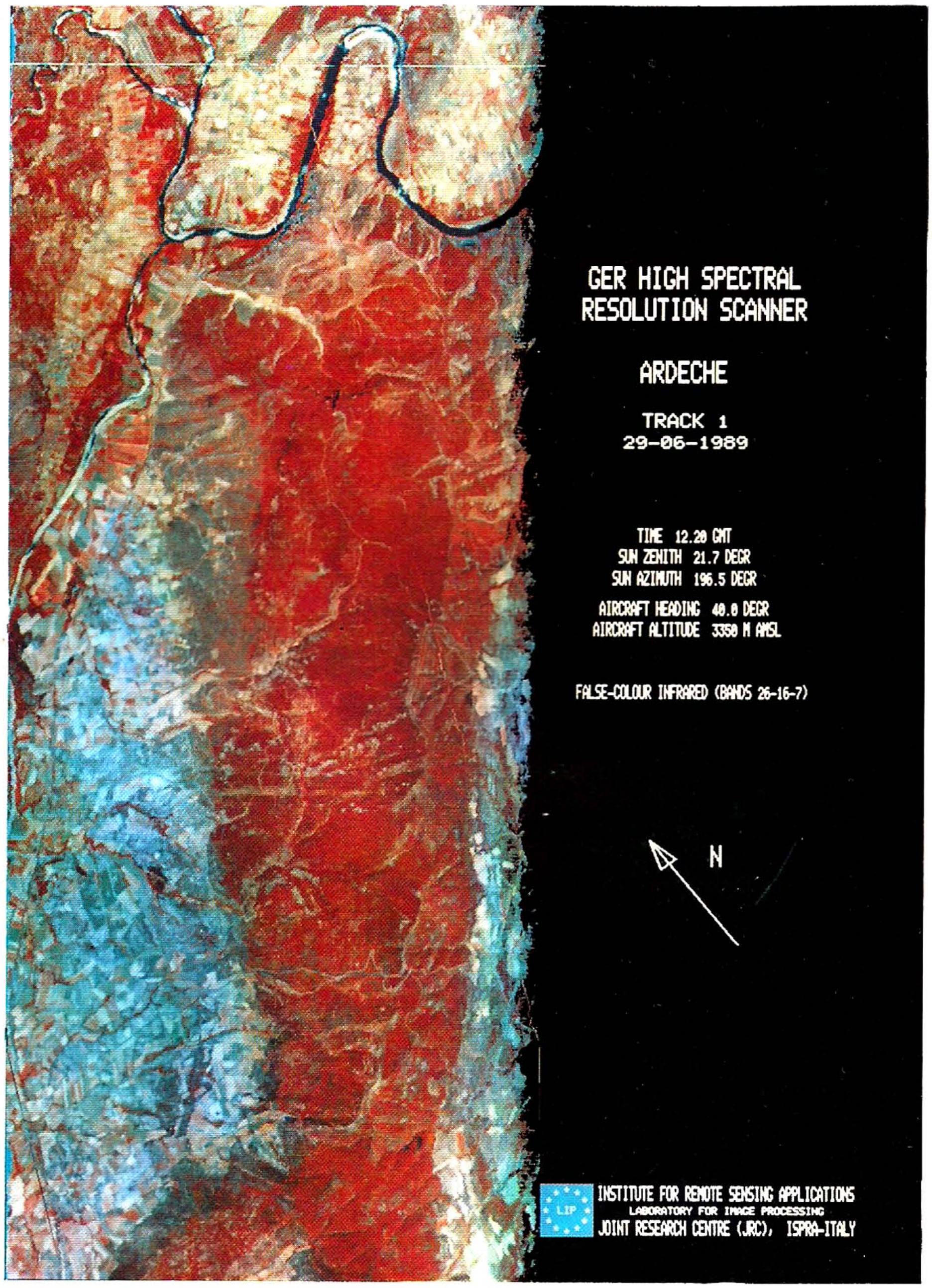

(Image Processing by LIP/IRSA, JRC Ispra)

Fig. 2. GERIS Track 1, acquired over the Ardèche High Resolution Spectrometry test site on 29 June 1989. False-colour representation of GERIS bands 26-16-7 (RGB).

pedological mapping campaigns were carried out in order to provide a detailed spatial data base for the analysis of the GERIS data (Negendank *et al.* 1990; Riezebos *et al.* 1990).

4. RADIOMETRIC CHARACTERISTICS OF THE GERIS DATA

An adequate analysis of imaging spectrometer data requires a thorough wavelength and radiometric calibration, and a converison of the data to reflectance factors so that individual spectra can be compared directly with laboratory data or spectral field measurements.

The atmospheric correction model which was used throughout this study is based on the formulation of radiative transfer as developed from Tanré *et al.* (1979, 1981, 1987), and it provides corrections for atmospheric absorption, scattering and pixel adjacency effects. It directly relates the apparent at-sensor reflectance ρ^* to the target reflectance factor ρ_t with

$$\rho^* = t_g(\mu) \{ \rho_{at} + \frac{T(\mu_0)\ [t_d(\mu)\ \rho_t + t_s(\mu) < \rho >]}{1 - < \rho > s} \} \quad (4.1)$$

where $< \rho >$ is the background contribution to the reflectance, and s is the spherical albedo; ρ_{at} denotes the intrinsic atmospheric signal component, $T(\mu_0)$ the total downward, $t_d(\mu)$ the diffuse and $t_s(\mu)$ the scattered upward transmittance; $t_g(\mu)$ gives the upward gaseous transmittance (Tanré et al. 1987). The apparent reflectance ρ^* at the airborne sensor is obtained from

$$\rho^* = \frac{\pi\ L\ d^2}{E_0\ T(\mu_0)\ t_g(\mu_0)\ \mu_0} \quad (4.2)$$

E_0 denotes the extraterrestrial solar irradiance [$mW/cm^2/\mu m$], L the upwelling radiance [$mW/cm^2/sr/\mu m$] measured at the sensor, μ_0 is the cosine of the solar zenith angle θ_0, and d is a correction coefficient which accounts for the daily variation in the sun-to-earth distance. In this case, $T(\mu_0)$ and $t_g(\mu_0)$ give the downward transmittances between the top of the atmosphere and the aircraft.

Diffusion and absorption processes are assumed to be independent. Upward and downward transmission coefficients are therefore easily derived by introducing the auxiliary quantity of optical thickness τ which measures the total extinction of a light beam due to molecular (τ_r) and aerosol scattering (τ_a) passing through an airmass. The absorbing atmospheric gases (H_2O, O_3, CO_2, O_2) are assumed to condense at the top of the atmosphere and at the top of the layer between the surface and the sensor altitude. Atmospheric path radiance (atmospheric reflectance) can optionally be evaluated according to the single scattering approximation (Gordon 1981) or to Sobolev's approximate solution of multiple scattering (Sobolev 1963).

The method has been exhaustively tested with TM and SPOT data, and it has proven its capability for retrieving ground reflectance factors with an average error of ± 0.015 (Hill and Sturm 1990; Hill and Aifadopoulou 1990). For the correction of data sensed at different altitudes the model had to be modified in order to approximate the atmospheric extinction processes as a function of altitude (Guzzi *et al.* 1987).

4.1 *GERIS Spectral Band Position*

A comparison of the GERIS band set to LOWTRAN standard atmospheric data reveals that numerous spectral channels are susceptible to significant gaseous absorption due to atmospheric water vapour, oxygen and carbon dioxide (Fig. 3). This must be accounted for in the atmospheric corrections, but the positions of known absorption features, such as the narrow O_2- (0.760 µm) or CO_2-absorption bands (2.005, 2.050 µm), can also be used to check the wavelength positions of the GERIS bands (Kruse *et al.* 1990). Atmospheric H_2O absorption bands in the visible part of the spectrum (0.720, 0.815 µm) are less reilable since their magnitude may vary according to the actual amount of water vapour present in the atmosphere.

GERIS raw spectra (expressed in counts), however, do not exhibit pronounced effects of these atmospheric absorption features. Therefore the center wavelength provided by GER corporation were only slightly modified for the VIR/NIR spectrometer by using known ground reflectance features (Lehmann *et al.* 1989).

4.2 *Spectral Bandwidth and Radiometric Calibration*

The radiometric in-flight calibration of the GERIS instrument was evaluated separately for each spectrometer module (VIS/NIR, SWIR I & SWIR II). As primary reference scene, the GERIS data set acquired over Freiburg (FRG) was selected. This data set covers a calibration site (sandy soccer field), were numerous radiometric ground

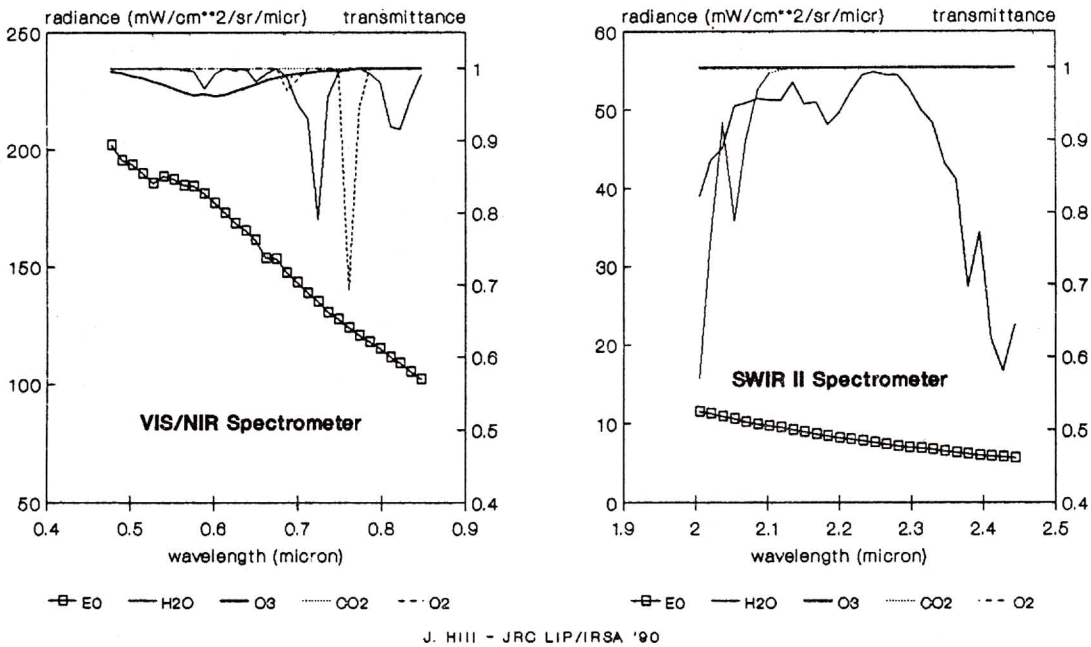

Fig. 3. Solar Exoatmospheric Irradiance and Atmospheric Gaseous Absorption in the GERIS Spectral Bands (Atmospheric Data from the LOWTRAN Mid - Latitude Summer Standard Atmosphere).

measurements with Exotech 100 A, SE-590 (Maracci *et al.* 1989) and IRIS MARK IV (Bach and Mauser 1989) field spectrometers have been carried out contemporarily to the GERIS overpass of 16 June 1989. For the purpose of verification, GERIS data from the Ardeche flight (29 June 1989) were used which also cover a suitable calibration site, but were acquired during less favourable atmospheric conditions (presence of some alto-cirrus clouds). GERIS data acquired over the northern Adriatic Sea (26 May 1989) completed the set of imagery used for this study.

For all GERIS scenes, atmospheric gaseous absorption was accounted for by using the default values of the LOWTRAN mid latitude summer atmosphere, the aerosol optical depth during the GERIS overpass at Freiburg (FRG) was derived from a series of contemporarily acquired measurements of atmospheric beam transmittance (Maracci *et al.* 1989). With an estimated horizontal visibilty of about 34 km, the computed aerosol optical depth corresponds quite well to the atmospheric conditions being reported for this GERIS flight (G. Maracci, pers. communication).

4.2.1 The GERIS VIS/NIR spectrometer (0.477-0.848 μm). The reconstructed in-flight calibration for the GERIS VIS/NIR spectrometer (channel 1-31) is based upon a reference reflectance signature of the sandy soccer field at Rothaus (Freiburg FRG) which was derived from averaging the ground measurements acquired with both SE-590 and IRIS MARK IV radiometers. In the GERIS data, this target is represented by 15 "pure" pixels.

The use of pre-flight calibration data as provided from GER Corporation produces reflectance factors which are generally lower than the ground measurement, and the spectral bands being affected from the atmospheric H_2O-, and especially O_2-absorption appear to be excessively overcorrected. These erroneous reflectance peaks do not appear when the effects of atmospheric gaseous absorption are completely excluded from the radiative transfer calculations (Fig. 4). It is therefore concluded that, in addition to an apparent decrease of the system sensitivity, the GERIS VIS/NIR bandpasses are not sensitive to narrow atmospheric absorption features. In case of the water vapour absorptions, this effect might be attributed to an extremely low H_2O-content of the actual atmosphere. But the evidence of a strong overcorrection at the wavelength of the O_2-absorption (0.762 μm) leads necessarily to the conclusion that the bandwidth of the GERIS VIS/NIR spectrometer is broader than specified.

An estimate of the actual bandwidth was obtained by comparing the results of radiative transfer calculations with varying bandwidth (12 - 60 nm) to a reference signature which was obtained for a 12-nm band located at 0.746 μm,

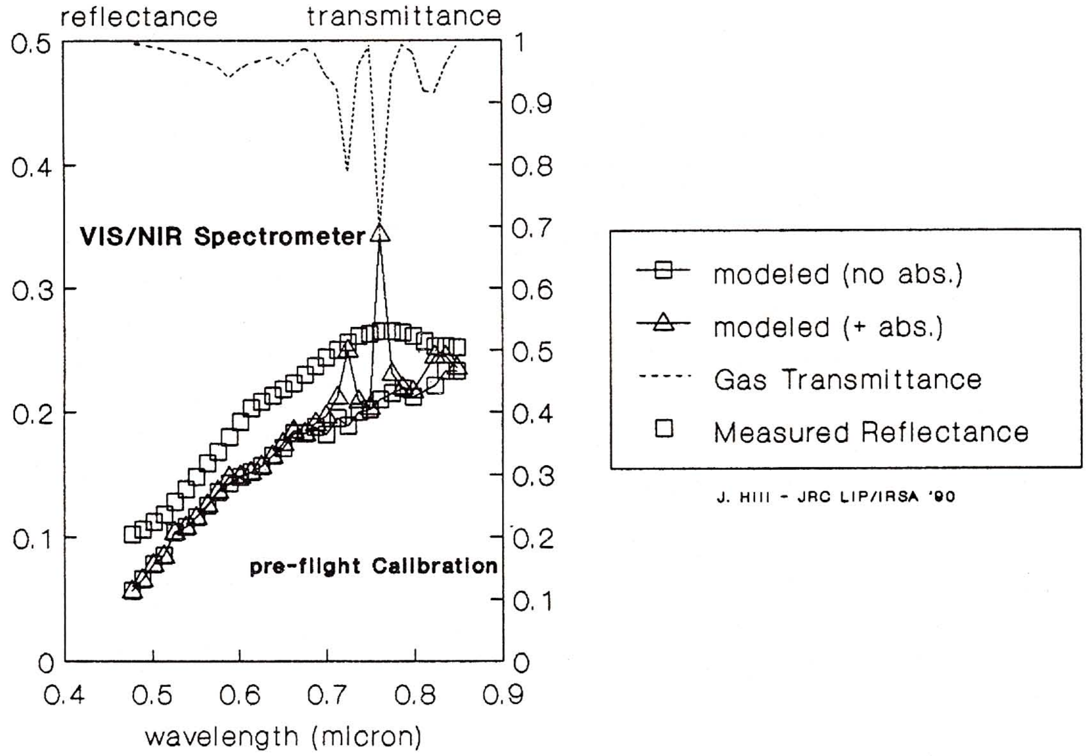

Fig. 4. GERIS Freiburg 13 June 1989: Measured and Modeled Reflectance (Pre-Flight Calibration) of the Calibration Target (Sandy Soccer Field, Rothaus, FRG). The Atmospheric Gaseous Transimttance Corresponds to the Nominal Width of The GERIS VIS/NIR Bands (12.3 nm).

TABLE 3
ESTIMATION OF GERIS VIS/NIR BANDWIDTH AT 0.762 μM (O_2-ABSORPTION)

λ $\Delta\lambda$	746 nm 12 nm	762 nm 12 nm	762 nm 20 nm	762 nm 30 nm	762 nm 40 nm	762 nm 50 nm	762nm 60 nm
ρ_r/ρ_s	1.0	0.59	0.72	0.82	0.86	0.89	0.90

just outside the O_2-absorption (Table 3). The resulting ratios of reference (ρ_r) and simulated (ρ_s) reflectance factors indicate that the effective bandwidth in the VIS/NIR spectrometer amounts to at least 50 nm, which is probably due to either mechanical vibrations or a defocussing of the respective sensor array (R. Richter, DLR, Oberpfaffenhofen, FRG, pers. communication).

4.2.2 The GERIS SWIR I spectrometer (1.44-1.80 μm). The first GERIS short-wave infrared spectrometer (channel 32-35) provides data only within four rather broad spectral bands (120 nm), two of which extend into the atmospheric water vapour absorption bands around 1.35 and 1.84 μm. Although the respective image data appear very noisy (despite the broad spectral bandwidth ?) approximative calibration adjustments could be performed with respect to the Freiburg calibration site.

4.2.3 The GERIS SWIR II spectrometer (2.005-2.443 μm). The short-wave infrared spectral region between 2.0 and 2.5 μm is especially important for the observation of rock and soil constituents (Hunt and Salisbury 1970, 1971 Hunt *et al.* 1971; Geerken and Kaufmann 1989). In order to fully exploit the diagnostic information being provided from the third GERIS spectrometer (channel 36-63), a very precise adjustment of the in-flight calibration gains is required. The Freiburg calibration site, however, proved to be not sufficiently homogeneous for assessing the calibration gains of this spectrometer, due to the strong spectral contrast between dry and partially irrigated sand, and an artificial calibration target which had been deployed on his sand surface during the GERIS overflight. We therefore selected several large, predominantly bare soil surfaces for which comparisons to radiometric field measurements were possible.

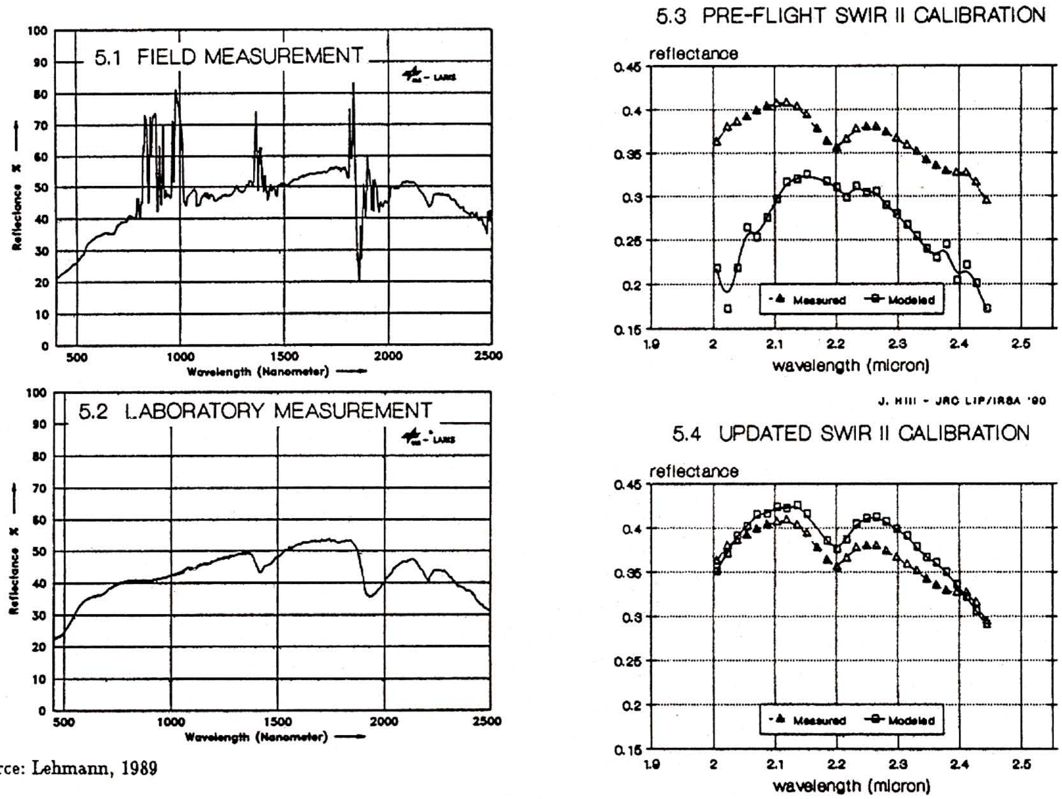

Source: Lehmann, 1989

Fig. 5. Ardèche Calibration Site (Domaine du Rouret): Ground and Laboratory Measurements Performed with the GER IRIS Mark IV Spectroradiometer (left) and the Comparison of using Pre- and In-Flight Calibration Data for Computing GERIS-based Reflectance Factors in the SWIR II Range (right).

The reconstructed in-flight calibration gains were independently assessed by computing spectral reflectance signatures for targets being included in the GERIS Ardèche data set. For this comparison, we refer to the respective calibration site ("Domaine du Rouret") which consists of a sufficiently large (60 x 80 m^2), flat, unvegetated and homogeneous surface, covered with small size quartz gravel. Accessory mineral constituents are kaolinite, illite and some minor amounts of calcite (Negendank *et al.* 1990). The ground - and laboratory - measured reflectance signature accordingly exhibits a pronounced absorption feature at 2.2 µm, and a shoulder is developed at about 2.35 µm (Fig. 5.1-5.2).

The updated calibration gains produce a reflectance signature which is in good agreement to the averaged ground and laboratory measurements, while the use of pre-flight constants indicate some radiometric disortions (i.e. wavelength shift of the 2.2 µm absorption feature) and a reduced sensivity of the SWIR II sensor array (Fig. 5.3-5.4). A modest overcompensation of atmospheric CO_2-absorption can be perceived in band 39 (2.054 µm) (Fig. 5.4). This might suggest that the actual bandwidth is somewhat broader than specified, but a precise quantification appears to be difficult. Therefore pre-flight specifications of band position and width have been maintained.

4.3 *GERIS Across-Track Radiometry*

While radiometric across-track effects are normally neglected for sensors with narrow fields of view (TM, SPOT), they should be accounted for in the atmospheric correction of images which have been acquired with large scan angles, such as the GERIS data (± 45 degrees). The evaluation of atmospheric path radiance must therefore incorporate the sun-target-sensor detection geometry. This requires, for each pixel position, the calculation of the backscattering for angle ψ

$$\cos\psi = -\cos\theta\cos\theta_0 - \sin\theta\sin\theta_0\cos(\varphi - \varphi_0) \qquad (4.3)$$

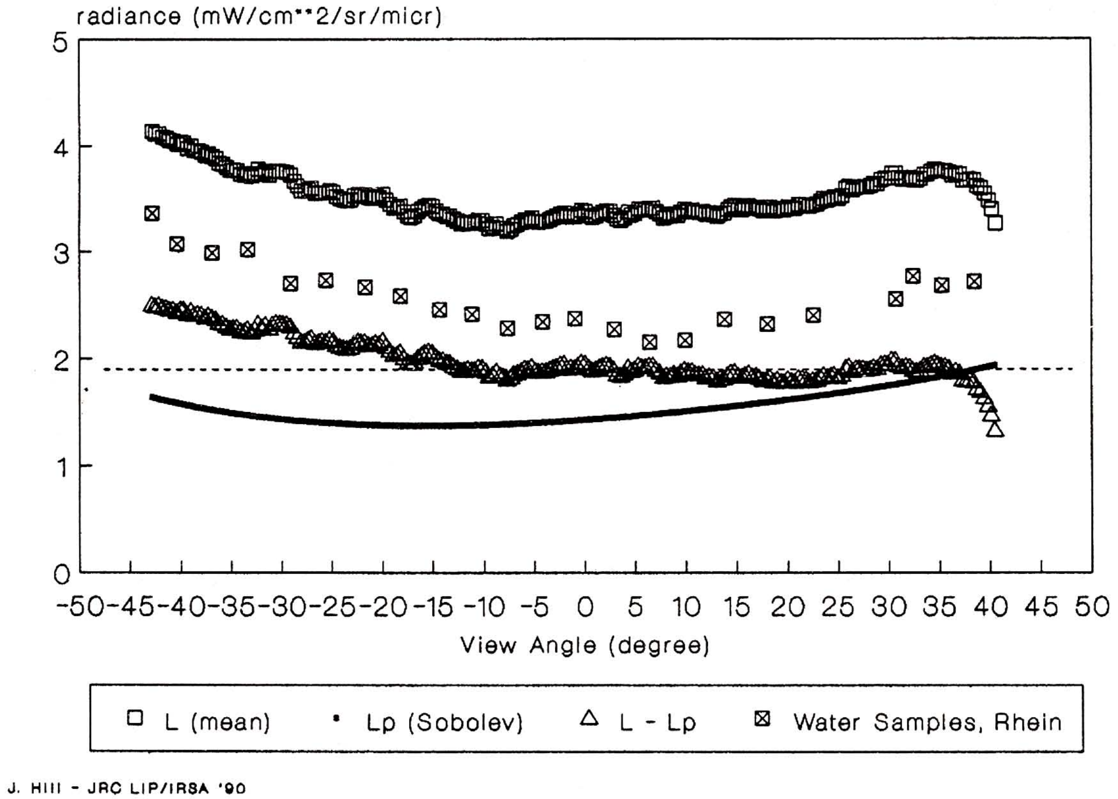

Fig. 6. Freiburg, 13 June 1989: GERIS Across-Track Radiometry as Derived from Along-Track Averaging and a Series of Water Samples from the River Rhein (Channel 1).

which, in conjunction with the corresponding phase functions

$$P_r(\psi) = 0.75\ (1 + \cos^2 \psi) \qquad (4.4)$$

for molecular, and a two-term Henyey-Greenstein approximation

$$P_a(\psi) = \frac{(1-g_1^2)\,\alpha}{(1+g_1^2-2g_1\cos\psi)^{1.5}} + \frac{(1-g_2^2)\,(1-\alpha)}{(1+g_2^2+2g_2\cos\psi)^{1.5}} \qquad (4.5)$$

for aerosol scattering, defines the amount of downwelling sun-light being scattered into the sensor's field of view; θ_0 and θ denote the sun and sensor zenith angles, $(\varphi - \varphi_0)$ gives the difference in azimuth of the sun and sensor planes. Depending on the sun-target-sensor geometry, the modeled atmospheric path radiance typically exhibits an asymetric variation in across-track direction.

Ideally, the actual within-scan radiometry of an image data can be assessed by extracting the spectral response from a target which does not change its reflectance properties across the whole imaged swath (such as the river Rhein in the Freiburg scene), or, assuming that local target variations average out over the whole image, by computing the respective column means (along-track averaging).

Both methods were applied to the GERIS data set from Freiburg, and both locally extracted target signatures from the river Rhein and the along- track averaged scene radiometry consistently emphasize an asymmetric variation of the across-track radiometry. The modeled path radiance, however, corresponds only to that part of the scene with $-20 < \theta > 0$ (Fig. 6). The same analysis was also performed using data from the GERIS flight over the northern Adriatic Sea. Depending on the type of parameters used in the two-term Henyey-Greenstein approximation of the aerosol scattering phase function (i.e. continental, maritime aerosol), the apparent across-track radiometric effects could be quite efficiently corrected (Fig. 7).

It was therefore concluded that the GERIS instrument does not produce pronounced radiometric artifacts within a scan line, except a rapid decrease of the signal level at the

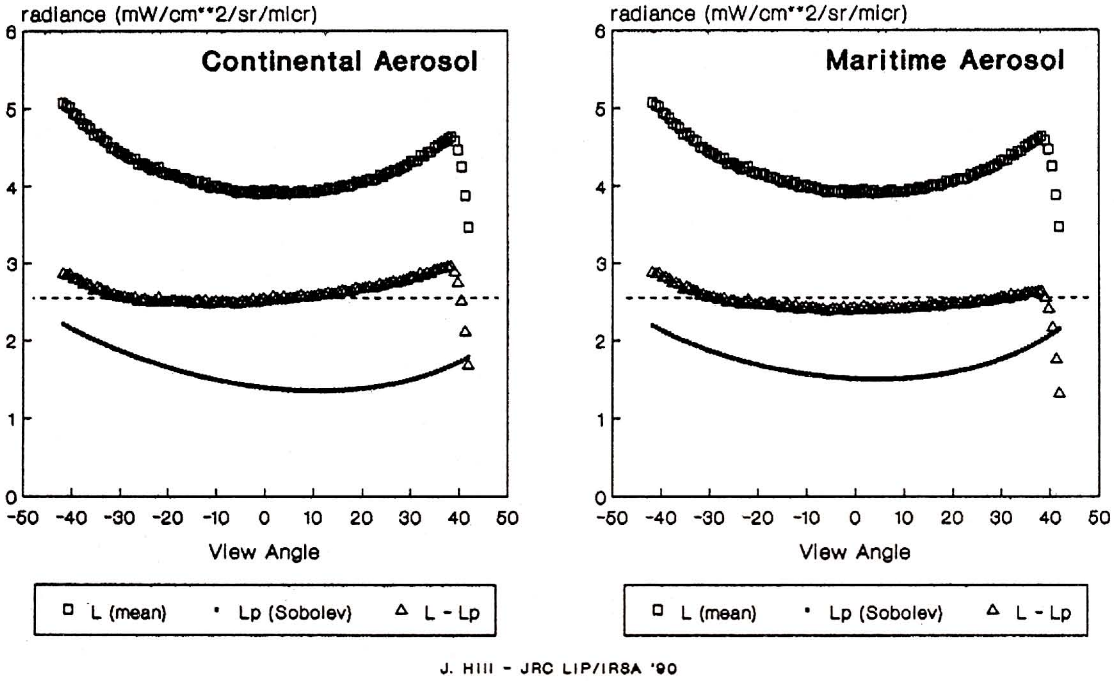

Fig. 7. GERIS Adria 16 May 1989, Channel 1: Modelistic Corrections of the Across-Track Radiometry Using Standard TTHG Aerosol Phase Functions.

end of each GERIS scan (Fig. 6,7). Wether this effect is due to a dark signal reference panel which existed in earlier verisons of the instrument (Lee *et al.* 1990), could not be verified.

The feasibility of correcting radiometric across-track distortions within the radiative transfer calculations seems to depend mainly on the correspondence between the approximated aerosol phase functions and the type of aerosol being present during the overflight.

It may appear more appropiate to correct the radiometric across-track effects by an image-based normalization to at-nadir conditions. Suitable weighting functions can be easily derived by fitting polynomials (typically of second order) to the along-track averaged column means. However, if the column means are biased due to the dominance of specific cover types within a scene, there is no other solution than using available standard phase functions within modelistic corrections.

4.4 *Instrumental Noise*

Instrumental noise problems are present in most imaging spectrometers which operate in the short-wave infrared spectral region (Conel *et al.* 1987; Vane 1987; Clark *et al.* 1988). The signal-to-noise ratio of the GERIS spectral channels was aproximately assessed by computing the ratio (μ/σ) of mean μ and standard deviation σ for several homogeneous target areas (25-50 pixels) of different brightness level.

Given the low reflectance of water, these estimates reveal a signal-to-noise ratio in the VIS/NIR spectrometer that is generally below 10:1. Over typical land surfaces (i.e. bare soils with $0.1 < \rho < 0.4$) it varies between 15:1 and 45:1 (VIS/NIR), which is still below the nominal values given by GER Corporation.

In the SWIR II spectrometer we find a wavelength dependency such that the signal-to-noise ratio deteriorates with decreasing radiance levels (due to atmospheric absorption). Given a target reflectance level between 0.35 and 0.50, the best signal-to-noise ratio is found in GERIS bands 40-50 (S/N $\cong$ 25:1), but S/N-values may decrease to about 10:1 in bands 36-38 and 55-63.

Some additional information noise is due to band-dependent smear effects which occur in the GERIS SWIR II spectrometer. Given the construction principles of the GERIS scanner, such effects can be explained with

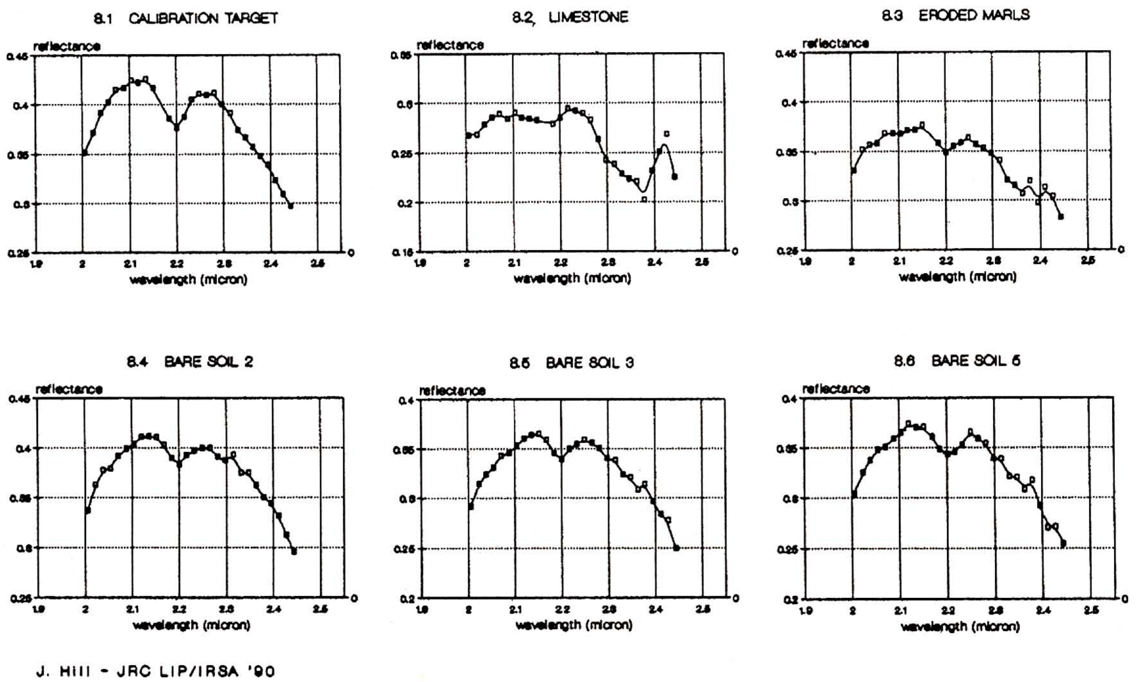

Fig. 8. GERIS Ardèche, 29 June 1989: Short-Wave Infrared Reflectance Signatures from Typical Ground Targets in the Study Site.

TABLE 4

MAJOR MINERALS DETECTED IN THE VIS/NIR AND SWIR SPECTRAL REGION

Wavelength (μm)	Major Minerals Detected	
0.40–1.20	Transition Elements, Fe, Mn & Ni Oxides Haematite, Goethite, Lepidocrocite REE–bearing Minerals	
1.30–2.50	Hydroxides, Carbonates & Sulphates	
1.47–1.82	Sulphates	– Alunite
1.47–1.76	Sulphates	– Jarosite
2.16–2.24	Al–OH Minerals	– Muscovite, Kaolinite – Dickite, Pyrophyllite – Smectite, Illite
2.24–2.26	Si–OH Minerals	– Opaline Silica
2.24–2.30	Fe–OH Minerals	– Jarosite, Hectorite, Saponite
2.30–2.40	Mg–OH Minerals	– Chlorite, Talc, Epidote – Amphibole
2.32–2.35	Carbonates	– Calcite, Dolomite, – Magnesite, Siderite

Source: Huntington et al., 1989

misalignments of individual detectors, or amplifier time-constant differences (positioning of individual pre-amplifiers). The latter appeared to be the reason for similar misregistrations which affected the first GERIS flight model (Lee *et al.* 1990).

5. SIGNATURE EXTRACTION AND PRELIMINARY THEMATIC ANALYSIS

The main advantage of imaging spectrometry is the improved direct identification of surface materials, using the quantifiable wavelength dependence of spectral reflectance. In the Ardèche High Resolution Spectrometry Experiment, the single components of soils and rocks, the minerals, are main targets which we want to identify.

Spectral absorption, reflection and emission features of rocks and soils originate from charge transfer and electronic transitions in the transition elements, overtone bending-stretching vibrations in hydroxyl and carbonate-bearing materials and fundamental Si-O vibrations in silicate materials (Hunt and Salisbury 1970, 1971; Hunt *et al.* 1971).

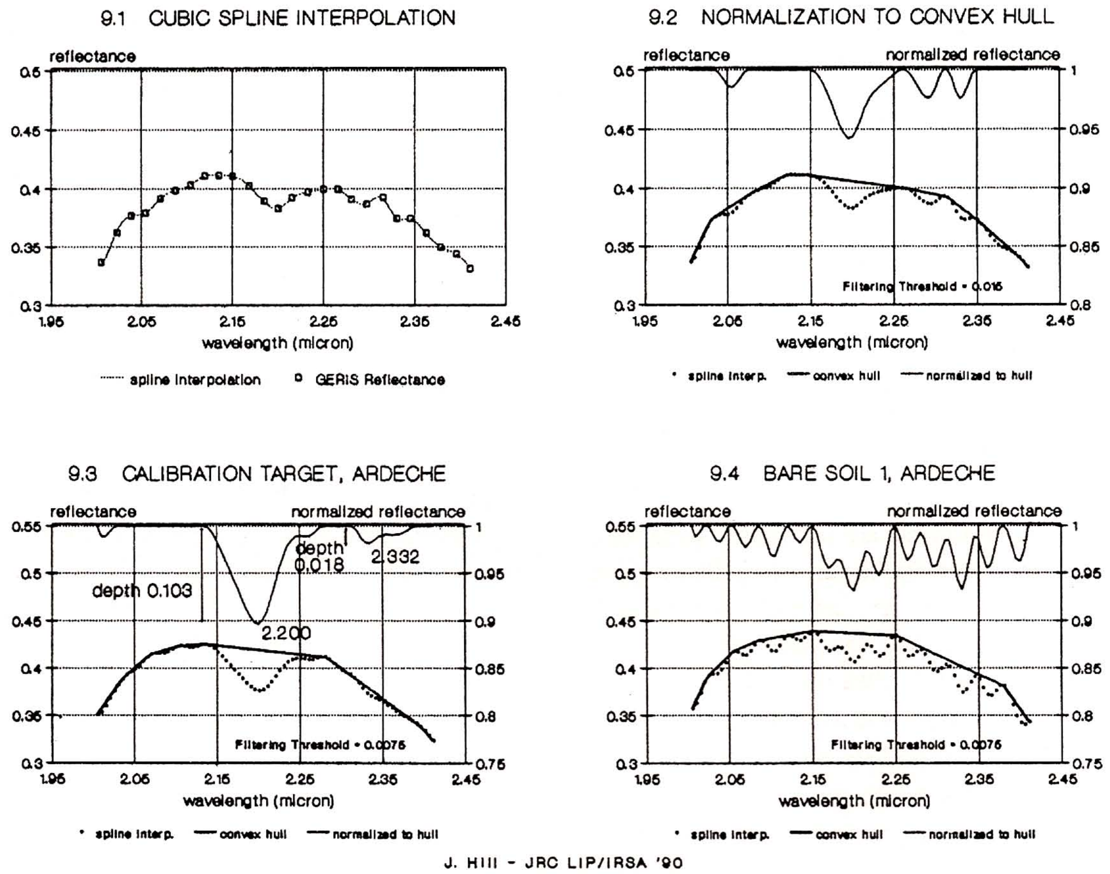

Fig. 9. GERIS Ardèche, 29 June 1989: Automatic Detection of Spectral Absorption Features by Removing a Spectral Continuum (Convex Hull).

Although not all minerals can be identified by these means (Table 4), we expect to recognize such surface features which can be used to more precisely characterize processes of land degradation and soil erosion. The characteristics that permit identification of spectra are associations of wavelengths of absorption or emission depth and absorption width at a certain depth (Huntington *et al.* 1989). Detection algorithms therefore concentrate on automatically locating such features at definite wavelengths, and on assessing their magnitude.

In this preliminary data analysis it was first attempted to verify whether the available GERIS spectra do in fact provide diagnostic information related to the dominant rock and soil units in the test site.

The GERIS reflectance signature of the Ardèche calibration site was chosen as reference spectrum which, in accordance with the spectral field and laboratory measurements, exhibits a pronounced absorption feature at 2.2 µm (Fig. 8.1). It results from the X-ray diffraction that this absorption is related to the presence of Al-OH bearing minerals such as kaolinite and illite (Negendank *et al.* 1990). In comparison to this reference spectrum, GERIS spectra from areas of widely exposed limestone show the spectral characteristics of CO_3 bearing standard minerals with absorption features around 2.18 µm, 2.30 and, somewhat noisy, at 2.35/2.38 µm (Fig. 8.2). It also corresponds to the results of the XRD analysis (presence of kaolinite and calcite in the parent rock) that GERIS spectra from heavily eroded marls reveal diagnostic absorption features which relate to both Al-OH and CO_3 bearing minerals (Fig. 8.3) and similar mixtures of mineralogical constituents consistently appear to be present in the fluvisols from the flood plain of the river Chassezac (Fig. 8.4 to 8.6)

These results confirm that the second GERIS shortwave infrared spectrometer (2.0-2.5 µm) provides the potential to distinguish minerals such as phyllosilicates and carbonates. This capability is considered important for assessing vegetation-soil mixtures and a more precise analysis of exposed soils in land degradation approaches.

The automatic detection of such absorption features will of course be affected from the sensor noise, especially when the magnitude of this noise is in range of the respective absorption maxima. In this preliminary thematic evaluation, it was attempted to automatically extract absorption features from GERIS SWIR II data by normalizing the reflectance signatures to a reference continuum (convex hull). In order to more precisely determine the wavelength position of absorption maxima, in a preparatory step almost continuous spectra (5 nm intervals) were approximated by applying a cubic spline interpolation to the original GERIS signal (9-25 pixel averages). This interpolated signal is then used to construct the convex hull, and the automatic detection algorithm uses the signature which is obtained by removing this continuum (Fig. 9.1, 9.2).

Once noise-related artifacts are removed, this detection algorithm can automatically identify spectral absorptions and provide descriptive parameters such as depth of the feature and full width at half the maximum depth (Fig. 9.3). The method has to fail when noise effects (i.e. due to the smearing effects) deteriorate the available spectral information. This may especially affect relatively small spatial features with a strong spectral contrast to their surroundings (Fig. 9.4).

The application of such or similar algorithms (i.e. absorption depth mapping, spectral unmixing) within a pixel-based treatment of GERIS scenes therefore appears difficult, unless advanced pre-processing methods are applied to reduce noise and improve the band-to-band correspondence within the GERIS short-wave infrared spectrometer.

6. CONCLUSIONS

GERIS data acquired during the EISAC '89 campaign over several european test sites suffer from numerous radiometric defects such as

- bandwidth deterioration of up to 50 nm in the VIS/NIR spectrometer
- significant differences between pre- and in-flight instrument calibration (all three spectrometers)
- moderate to bad signal- to- noise ratio in all spectrometers

In-flight calibration gains and offsets could be reconstructed by using radiometric ground measurements and suitable radiative transfer calculations, and these reconstructed calibration gains appear to be stable for GERIS data from different test sites. The risk of introducing artifacts during this reconstruction process, however, may require additional verification by radiometric ground and laboratory measurements of suitable reference surfaces (i.e. bare soils).

The use of image spectra from the GERIS VIS/NIR spectrometer seems to be limited due to the effective bandwidth which amounts to at least 50 nm. It is questionable whether methos for assessing the so-called vegetation red edge (fitting of inverted gaussian functions, estimating its slope) can be successfully applied, since GERIS image spectra, due to the increased bandwidth, considerably smooth significant spectral features such as the green reflection peak, the chlorophyll absorption maximum or the transition to the near-infrared plateau.

There is strong evidence that position and width of the spectral bands in the GERIS SWIR II spectrometer (channel 36-63) are close to or even within the specifications. Mineral absorption features in soils and rocks could be identified once stable target statistics (9 to 25 pixel averages) were used. Due to the moderate signal-to-noise ratio in all GERIS spectrometers, it remains uncertain whether pixel-by-pixel evaluations such as spectral unmixing or feature mapping will be feasible without the prior application of advanced noise-removal procedures.

ACKNOWLEDGMENTS

I wish to acknowledge the efforts of my colleague W. Mehl in extending the existing LIP image processing software for handling and display of high resolution imaging spectrometer data. Many thanks go to J. Mégier (Head Laboratory for Image Processing) for his support of the current HRS research program in the Ardèche, to G. Maracci for the radiometric ground measurements, to B. Sturm for many discussions about the atmospheric corrections, and to M. Altherr for his assistance in GERIS data processing.

REFERENCES

Bach, H. and W. Mauser, 1989, "EISAC 1989. Report on the ground data collection test site Freiburg", Inst. Physical Geography, Dept. of Hydrology, Univeristy of Freiburg, FRG.

Clark, R.N., B.J. Middlebrook, G.A. Swayze, K.E. Livo, D.H. Knepper, T.V.V. King and K. Lee, 1988, "Calibration and evaluation of AVIRIS data: Cripple Creek in October 1987".

In: Vane, G. (ed.), *Proc. of the Airborne Visible/ Infrared Imaging Spectrometer (AVIRIS) performance evaluation workshop*, JPL Publication 88-38, 49-61.

Conel, J.E., R.O. Green, G. Vane, C.J. Bruegge, R.E. Alley and B.J. Curtiss, 1987, "Airborne Imaging Spectrometer-2: Radiometric spectral characteristics and comparison of ways to compensate for the atmosphere". In: Vane, G. (ed.), *Imaging Spectroscopy II, Proc. SPIE* 834, 140-157.

FAO, 1988, *FAO-Unesco soil map of the world*, Rome.

Gordon, H.R., 1981, "A preliminary assessment of the Nimbus-7 CZCS atmospheric correction algorithm in an horizontally inhomogeneous atmosphere". In: Grown, J.F.R. (ed.), *Oceanography from space*, (Plenum Press: New York, London).

Geerken, R. and H. Kaufmann, 1989, "Spectral effects of surface characters and rock accessories. A critical contribution to the applicability of high spectral resolution sensor data". *Proc. 9th EARSeL Symposium*, held at Espoo, Finland, 27 June - 1 July 1989, Commission of the European Communuties: Office for Official Publications, Luxembourg, EUR 21827, 501-511.

Guzzi, R., R. Rizzi and G. Zibordi, 1987, "Atmospheric correction of data measured by a flying platform over the sea: elements of a model and its experimental validation", *Applied Optics*, 26, 3043-3051.

Hill, J. and B. Sturm, 1991, "Radiometric Correction of multitemporal Thematic Mapper data for the use in agricultural land-cover classification and vegetation monitoring", *International Journal of Remote Sensing*, in press.

Hill, J. and D. Aifadopoulou, 1990, "Scene-based atmospheric correction of Thematic Mapper imagery acquired over the Ispra/Novara region (Italy) in 1988", Institute for Remote Sensing Applications, JRC Ispra, Technical Note.

Hunt, G.R. and J.W. Salisbury, 1970, "Visible and near infrared spectra of minerals and rocks: I. Silicate minerals", *Modern Geology*, 1, 183-300.

Hunt, G.R. and J.W. Salisbury, 1971, "Visible and near infrared spectra of minerals and rocks: II. Carbonates", *Modern Geology*, 2, 23-30.

Hunt, G.R., J.W. Salisbury and C.J. Lenhoff, 1971, "Visible and near infrared spectra of minerals and rocks: III. Oxides and hydroxides", *Modern Geology*, 2, 195-205.

Huntington, J.F., A.A. Green and M.D. Craig, 1989, "Identification - the goal behind discrimination. The status of mineral and lithological identification from high resolution spectrometer data: Examples and challenges", *Proc. IGARSS'89 Symposium*, 10 - 14 July 1989, Vancouver, Canada, vol.1, 6-11.

Kruse, F.A., K.S. Kierein-Young and J.W. Boardman, 1990, "Mineral mapping at Cuprite, Nevada with a 63-channel imaging spectrometer", *Photogrammetric Engineering and Remote Sensing*, vol.56, no.1, 83-92.

Lee, J.B., A.S. Woodyatt and M. Berman, 1990, "Enhancement of high spectral resolution remote-sensing data by a noise-adjusted principal components transform", *IEEE Transactions on Geoscience and Remote Sensing*, vol.28, no.3, 295-304.

Lehmann, F., S. Mackin, R. Richter, H. Rothfuss and A. Walbrodt, 1989, "The European Imaging Spectroscopy Campaign 1989 (EISAC) - pre- processing, processing and data evaluation of the GER airborne imaging spectrometer data". Progress report to the European Communities, JRC, Ispra, Institute for Optoelectronics, DLR - German Aerospace Research Establishment, Oberpfaffenhofen.

Lehmann, F. (ed.), 1989, "Reflexionsspektroskopische Labor- und Geländemessungen von Böden aus der Ardèche (Frankreich)", Final report study contract no.3740-89-06 ED ISP D, Institute for Optoelectronics, DLR - German Aerospace Research Establishment, Oberpfaffenhofen.

Mackin, S. and T.J. Munday, 1988, "Imaging spectrometry in environmental research and applications". Interim Report 1: Preliminary results from the analysis of GER-II imaging spectrometer data (Australia and the USA), Contr.No.: D/ER1/1/9/4 2051/40/RAE(F) BNSC, U.K.

Maracci, G., G. Andreoli, P. Grassi and B. Hosgood, 1990, "Ground truth radiometric measurements in Ardèche (F) in 1989", Institute for Remote Sensing Applications, JRC Ispra, Technical Note, T.N.I.90.04.

Maracci, G., B. Hosgood, G. Andreoli and P. Grassi, 1989, "European Imaging Spectroscopy Aircraft Campaign (EISAC'89). Ground truth radiometric measurements in the Upper Rhine Valley", Institute for Remote Sensing Applications, JRC Ispra, Technical Note, T.N.I.89.117.

Negendank, J.F.W., H. Baumann, H. Siemann and H.B. Brückner, 1990, "Geological mapping and mineralogical analysis of surface samples for soil erosion assessment with High Resolution Spectroscopy data (Ardèche), Final report study contract no.3790-89-08 ED ISP D, Inst. of Geology, University of Trier, FR Germany.

Riezebos, H.Th., S.M. de Jong, J.C. van Hees and P.B.M. Haemers, 1990, "Physiographic and pedological mapping for soil erosion hazard assessment (Ardeche test site)", Final report study contract no.3787-89-08 ED ISP NL, Inst. of Geographical Research, University of Utrecht, The Netherlands.

Sobolev, V.V., 1963, *A treatise on radiative transfer*, (Van Nostrand: Princeton).

Tanré, D., M. Herman, P.Y. Deschamps and A. de Leffe, 1979, "Atmospheric modeling of the background contribution upon space measurements of ground reflectance, including bi-directional properties", *Applied Optics*, 18, 3587-3594.

Tanré, D., M. Herman and P.Y. Deschamps, 1981, "Influence of the background contribution upon space measurements of ground reflectance", *Applied Optics*, 20, 3676-3684.

Tanré, D., P.Y. Deschamps, P. Duhaut and M. Herman, 1987, "Adjacency effects produced by the atmospheric scattering in Thematic Mapper data", *Journal of Geophysical Research*, 92, D10, 12000-12006.

Vane, G., 1987, "First results from the Airborne Visible/Infrared Imaging Spectrometer (AVIRIS)". In: Vane, G. (ed.), *Imaging Spectroscopy II, Proc. SPIE* 834, 166-174.

Vane, G. and A.F.H. Goetz, 1988, "Terrestrial imaging spectroscopy", *Remote Sensing of Environment*, 24, 1-29.